DETERMINING THE BULK CHEMICAL COMPOSITION OF CHONDRULES BY ELECTRON MICROPROBE: A COMPARISON OF DIFFERENT APPROACHES. Jana Berlin, Rhian H. Jones and Adrian J. Brearley, Department of Earth and Planetary Sciences, University of New Mexico, Albuquerque, NM 87131, U.S.A., e-mail: jberlin@unm.edu

Introduction: A precise knowledge of bulk chemical compositions of chondrules is not only essential for understanding the relationship between chondrules and matrix [*e.g.* 1], but also for constraining the chondrule forming mechanism [2]. Despite the given importance, relatively few data sets for chondrule bulk chemical compositions are available in the literature, especially for the most primitive chondrites [3]. Instrumental neutron activation analysis (INAA) and electron probe microanalysis (EPMA) are the two major methods used to obtain such datasets, but each technique has its disadvantage. Si cannot be measured by INAA and trace elements are difficult to obtain by EPMA. There is also some discussion on how representative the composition of a 2 dimensional section is versus the 3 dimensional composition [4,5]. Separating chondrules for INAA analysis is challenging, especially for meteorites with very small chondrules (*e.g.* CO chondrites). In such a case, EPMA is the most realistic routine method that can be used to obtain chondrule bulk compositions. In this abstract, we point out problems with various EPMA methods that have been used. We compare several different approaches for determining bulk compositions using EPMA, including: (1) broad beam or defocused beam analyses (DBA), (2) modal recombination analysis (MRA) using backscattered electron images and (3) MRA using element maps.

Sample and analytical conditions: We measured the bulk composition of a type I chondrule from the Vigarano (CV3) chondrite (Fig. 1). An accelerating voltage of 15 keV was used for all analyses. Table 1 shows the beam current and probe diameter utilized for defocused beam analyses and point analyses on the different phases. Element maps were obtained using a beam current of 30 nA. For MRA, the area % of the different phases were determined using Scion Image Software (http://www.scioncorp.com/frames/fr_scion_products.htm).

Table 1: Analytical conditions.

	Beam current	Probe diameter
Broad beam analyses	20 nA	50 µm
Olivine, pyroxene	20 nA	1 µm
Mesostasis	10 nA	10 µm
Metals, sulfides	40 nA	1 µm
Magnetite	20 nA	1 µm

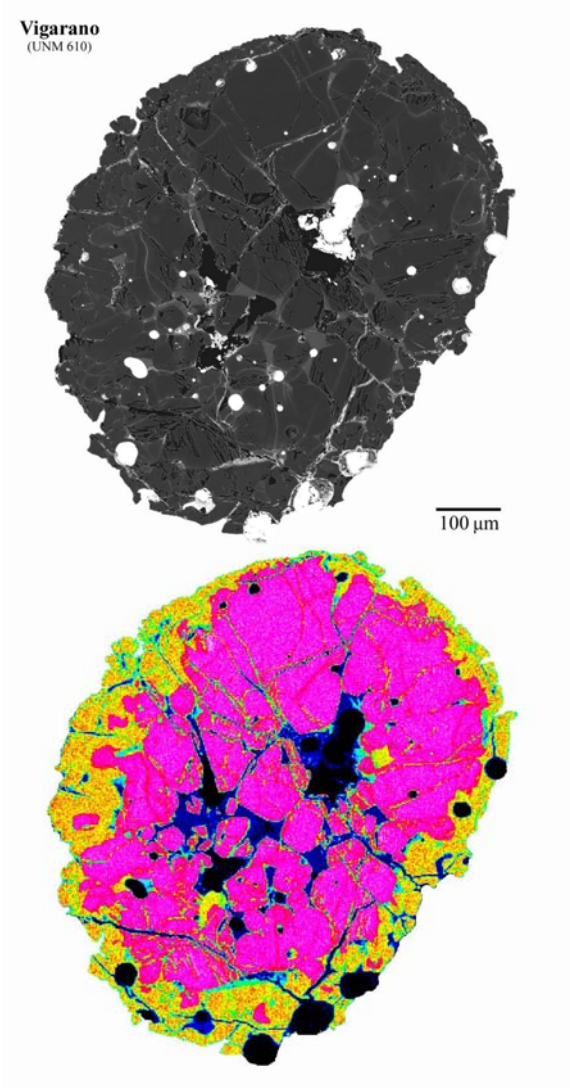

Fig. 1: Backscattered electron image and Mg map of the Vigarano chondrule for which data are presented. The Mg map is required to recognize the pyroxene rim.

Results: *(1.) Defocused beam analyses (DBA).* A grid of 74 analyses (100 µm apart) covered the entire chondrule. 43 analyses had an acceptable total (between 98 and 102 wt%). Low totals were obtained on spots where cracks or holes are present, whereas high totals correspond to mixed analyses (silicate + metal/sulfides). The bulk composition was calculated in 3 different ways (column 1a-c, Table 2).

For column 1a, the average of the 43 analyses with an acceptable total was calculated. For column 1b, 29 analyses with totals between 85 and 98 wt% as well as between 102 and 115 wt% were normalized to

100 % and averaged together with the 43 analyses from column 1a. This is not an ideal solution, especially for the mixed analyses, but it proved difficult to treat them in a more quantitative way. Because DBA are known to be fairly inaccurate [6], we corrected the bulk composition listed in column 1b with an unequal host-phase density correction factor as described by [6]. However, this was only possible because the modal abundances of the phases and their average elemental concentrations were exactly known from our modal recombination analysis (method 3). The result of the correction is shown in column 1c.

(2.) Modal recombination analysis (MRA) using back-scattered electron images (BSE). Because of the similar average atomic number of the phases, it was not possible to distinguish between olivine and pyroxene in the BSE image (see Fig. 1). For the mean composition of olivine/pyroxene, we used the average of 22 random points, 3 of which were pyroxene. Mesostasis and Ca-pyroxene could be identified easily. To discriminate between Fe,Ni-metal, sulfides, and magnetite, a second BSE image with lower brightness and higher contrast settings was taken (not shown). Average compositions of each phase obtained from point analyses were multiplied by the area % of the phase and summed up in order to obtain the bulk composition of the chondrule (column 2 in Table 2).

(3.) Modal recombination analysis (MRA) using element maps. Using element maps, 9 different phases could be identified: olivine, pyroxene, Na-rich and Na-poor mesostasis, Ca-pyroxene, kamacite, taenite, troilite and magnetite. The calculated bulk composition is shown in column 3 in Table 2.

Discussion: The results of the three different approaches are compared in Fig. 2, in which we normalize the various results to method 3. We consider our third method (MRA using element maps) the best possible approach when EPMA data must be used for bulk chondrule analysis, because all phases could easily be identified and analysed. DBA seem not as reliable as MRA. We find high Al and low Ti (Fig. 2) as also discussed by [6]. Our values for Mg, Si, Cr, Mn, and Na are very similar irrespective of the method used. Ca is low in method 2, because $CaCO_3$ veins (terrestrial alteration) were not taken into account. Fe, Ni, and S are very variable depending on the method chosen. DBA is the least reliable method for these elements. The DBA density correction is probably more useful for more fine-grained materials. Employing our third method, we are planning a more extensive survey of bulk chondrule compositions in primitive chondrites.

Table 2: Results of bulk chondrule analysis obtained by (1.) DBA (defocused beam analysis, for a, b, and c see text), (2.) MRA (modal recombination analysis) using BSE images and (3.) MRA using element maps for determining the modal abundances of the phases.

	1. DBA			2. MRA	3. MRA
	a	**b**	**c**	**[BSE]**	**[maps]**
Al	1.35	1.43	1.25	0.64	0.92
Ca	1.19	1.23	1.13	0.65	1.12
Ti	0.05	0.05	0.05	0.05	0.08
Mg	27.1	26.5	25.4	28.7	26.7
Si	20.0	19.6	18.7	19.9	20.9
Cr	0.46	0.46	0.45	0.36	0.41
Mn	0.04	0.04	0.04	0.04	0.04
K	0.022	0.023	0.023	0.016	0.016
Na	0.21	0.22	0.18	0.18	0.20
Ni	0.14	0.21	0.48	0.16	0.20
Fe	3.94	5.18	9.16	4.38	4.75
S	0.40	0.52	0.71	0.64	0.72

References: [1] Huss G. R. et al. (2005) In: *Chondrites & the protoplanetary disk*, 701-731. [2] Ciesla F. J. (2005) In: *Chondrites & the protoplanetary disk*, 811-820. [3] Jones R. H. et al. (2005) In: *Chondrites & the protoplanetary disk*, 251-295. [4] Hezel D. C. et al. (2005) *LPS XXXVI*, Abstract #2330. [5] Hezel D. C. (2005) *Paneth Kolloquium Nördlingen*, Abstract #006. [6] Warren P. H. (1997) *LPS XXVIII*, Abstract #1406.

Acknowledgements: J.B. thanks Jörg Fritz for all his help with the software and Mike Spilde for being such a great teacher for EPMA.

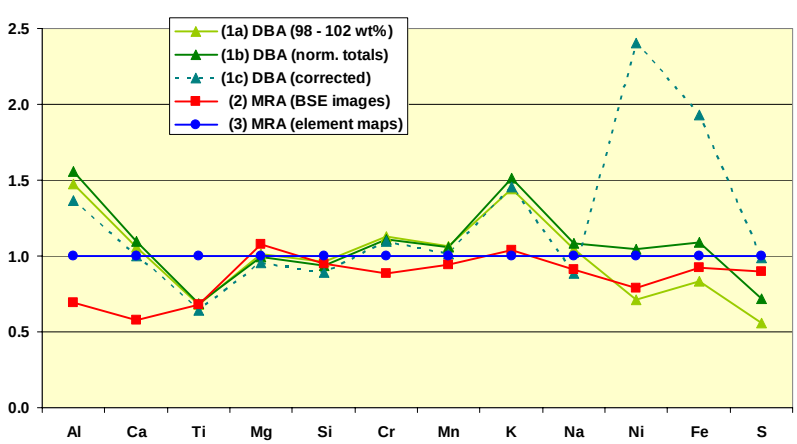

Fig. 2: Comparison of 3 different EPMA methods to obtain bulk chondrule compositions. Data are normalized to values obtained by method 3.